# N-WASP is a novel regulator of hair-follicle cycling that controls antiproliferative TGFβ pathways

**Tine Lefever[1,2,3], Esben Pedersen[1,2], Astrid Basse[1,2], Ralf Paus[4,5], Fabio Quondamatteo[6], Alanna C. Stanley[6], Lutz Langbein[7], Xunwei Wu[1], Jürgen Wehland[8], Silvia Lommel[9] and Cord Brakebusch[1,2,*]**

[1]Biomedical Institute and [2]BRIC, University of Copenhagen, 2200 Copenhagen, Denmark
[3]University of Ghent, 9052 Gent (Zwijnaarde), Belgium
[4]Department of Dermatology, Allergology and Venerology, University of Lübeck, 23538 Lübeck, Germany
[5]School of Translational Medicine, University of Manchester, Manchester, UK
[6]Department of Anatomy, National University of Ireland, Galway, Ireland
[7]German Cancer Research Center (DKFZ), Genetics of Skin Carcinogenesis (A110), 69120 Heidelberg, Germany
[8]Helmholtz Centre for Infection Research, 38124 Braunschweig, Germany
[9]Institute for Cell Biology, University of Bonn, 53121 Bonn, Germany
*Author for correspondence (cord.brakebusch@bric.dk)

*Accepted 15 April 2009*
*Journal of Cell Science 123, 128-140 Published by The Company of Biologists 2010*
*doi:10.1242/jcs.053835*

## Summary

N-WASP is a cytoplasmic molecule mediating Arp2/3 nucleated actin polymerization. Mice with a keratinocyte-specific deletion of the gene encoding N-WASP showed normal interfollicular epidermis, but delayed hair-follicle morphogenesis and abnormal hair-follicle cycling, associated with cyclic alopecia and prolonged catagen and telogen phases. The delayed anagen onset correlated with an increased expression of the cell-cycle inhibitor p21CIP, and increased activity of the TGFβ pathway, a known inducer of p21CIP expression. Primary *N-WASP*-null keratinocytes showed reduced growth compared with control cells and enhanced expression of the gene encoding the cell-cycle inhibitor p15INK4B, a TGFβ target gene. Inhibition of TGFβ signaling blocked overexpression of p15INK4B and restored proliferation of N-WASP-deficient keratinocytes in vitro. However, induction of N-WASP gene deletion in vitro did not result in obvious changes in TGFβ signaling or growth of keratinocytes, indicating that the in vivo environment is required for the phenotype development. These data identify the actin nucleation regulator N-WASP as a novel element of hair-cycle control that modulates the antiproliferative and pro-apoptotic TGFβ pathway in keratinocytes in vivo and in vitro.

**Key words:** N-WASP, Hair cycling, Keratinocytes

## Introduction

Dynamic actin assembly is crucial for various cellular processes such as protrusions of the plasma membrane, cytokinesis, endocytosis and vesicular transport (Pollard and Borisy, 2003). Crucial for many of these dynamic actin rearrangements is the actin-related protein (Arp)2/3 complex, which nucleates actin filaments. A prominent regulator of Arp2/3 activity is N-WASP (neuronal Wiskott-Aldrich syndrome protein), which binds both Arp2/3 via its CA domain and actin monomers through its WH2 domains, inducing the actin-filament-nucleating activity of the Arp2/3 complex (Millard et al., 2004). After binding, N-WASP captures the growing barbed ends of the filaments at the membrane surface, promoting elongation (Co et al., 2007). N-WASP activity itself is regulated by an intramolecular inhibitory interaction, which is relieved by binding of phospholipids such as phosphatidylinositol (4,5)-bisphosphate or the GTP-bound Rho GTPase Cdc42. In addition, other factors such as Nck, Grb2, Abi, Abp1 or WIP also interact with N-WASP and modulate its activity (Innocenti et al., 2005; Millard et al., 2004; Pinyol et al., 2007).

Different functions have been described for N-WASP in cultured cells. First, N-WASP was shown to regulate invadopodia (Mizutani et al., 2002). Second, both clathrin-dependent (Innocenti et al., 2005) and clathrin-independent endocytosis (Yarar et al., 2007) require N-WASP-mediated actin nucleation for optimal function. Third, knockdown of N-WASP distorts the organization of E-cadherin and F-actin at early cell-cell contacts in Caco-2 cells, suggesting a role of N-WASP in maintaining the structural integrity of epithelial tissues (Otani et al., 2006). Fourth, N-WASP was found in the nucleus, where it regulates RNA-polymerase-II-dependent transcription by interaction with the PSF-NonO complex, which controls transcription, RNA processing and DNA repair (Wu et al., 2006a). Finally, polymerization of nuclear actin has been reported to be promoted by N-WASP, which might affect chromatin remodeling and transcription (Wu et al., 2006a).

Not much is known about N-WASP function in vivo. Mice constitutively lacking N-WASP show severely delayed development and die before E12 with abnormalities in neural tube, heart and mesoderm differentiation (Lommel et al., 2001; Snapper et al., 2001). To better understand the function of N-WASP in the maintenance of epithelial cell-cell contacts (Otani et al., 2006), the regulation of gene expression (Wu et al., 2006a), and in epithelial tissue remodeling, we have generated mice with a deletion of the gene encoding N-WASP restricted to the skin epithelium.

Keratinocytes at various stages of differentiation are the main cellular constituents of epidermis and hair-follicle epithelium (Fuchs, 2007). The basal keratinocytes are attached to the basement membrane. If they lose contact to it, they stop proliferating and start towards terminal differentiation, which finally ends in the formation of the stratum corneum. This structure is composed of dead cell bodies and is part of the skin barrier that protects the body from dehydration, microbial invasion and other external stressors (Fuchs, 2007). Keratinocytes are connected to each other by desmosomes, adherens junctions and tight junctions, which are all crucial for skin integrity (Niessen, 2007).

Journal of Cell Science

Hair follicles emerge from the epidermis during embryogenesis in response to dermal signals involving different signaling pathways such as Wnt, BMP and FGF (Fuchs, 2007). Characteristic for hair follicles is their cyclic organ transformation, where a proliferation phase (anagen) alternates with an apoptosis-driven involution (catagen) phase, followed by a phase of relative quiescence (telogen). In mice, this hair cycle is highly synchronized during the first anagen, which is initiated at around P28 (Müller-Röver et al., 2001). How the timing of the 'hair cycle clock' that controls these transitions is regulated is only poorly understood, although several genes have been shown to influence the length and onset of the different phases of the hair cycle (Paus and Foitzik, 2004) and recent work has revealed that both intra- and extrafollicular oscillator systems drive hair-follicle cycling (Plikus et al., 2008). Due to this complex regulation, hair follicles are very sensitive to alterations in signaling pathways affecting cell growth and apoptosis. Also, they have long been recognized as an excellent model system for studying general principles of tissue remodeling and organ regeneration (Paus and Foitzik, 2004).

We show here that loss of N-WASP in skin epithelium causes a phenotype that is quite unique and different from what has been reported for the mutant of the N-WASP activator Cdc42 – inhibition of hair growth due to increased TGFβ signaling, which correlates with a delayed anagen entry of the N-WASP-deficient hair follicles. The data reveal an unexpected link between a major regulator of Arp2/3-mediated actin nucleation and TGFβ signal transduction and indicate N-WASP as a novel and functionally important regulator of hair-follicle cycling. Thus, we describe a new pathway, showing how regulation of the actin cytoskeleton can control epithelial organ regeneration.

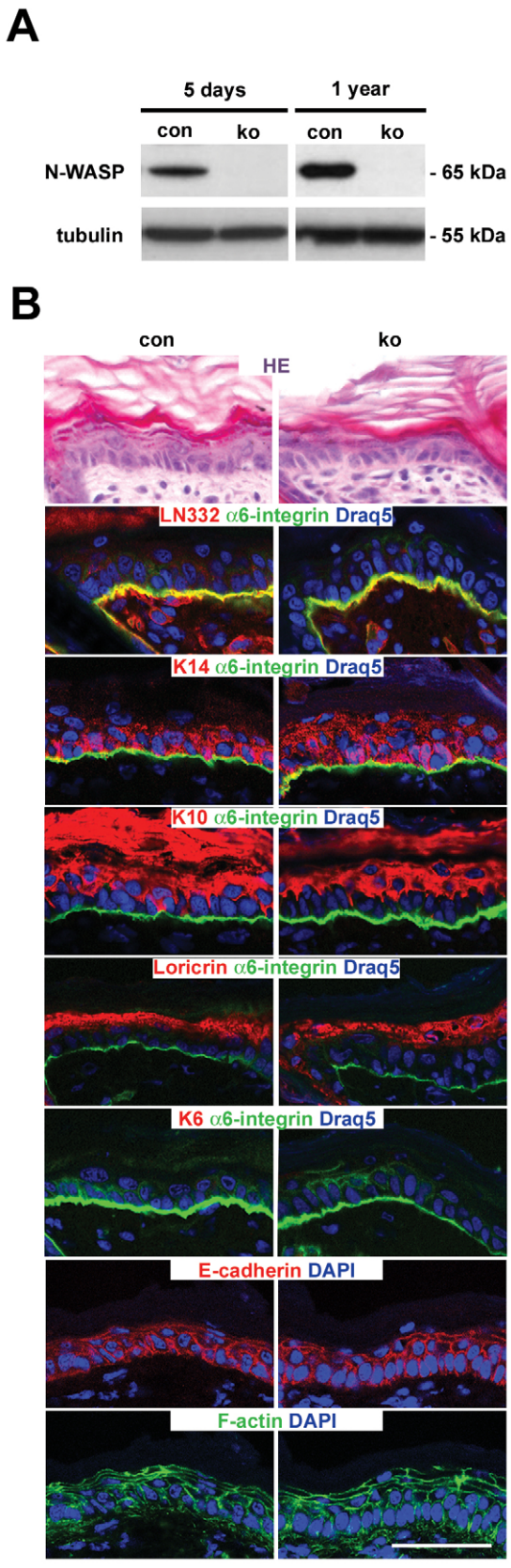


## Results

### N-WASP fl/fl K5 mice show normal epidermal development and maintenance

Mice with a keratinocyte-restricted deletion of the gene encoding N-WASP (N-WASP fl/fl K5) were born at Mendelian ratio and showed an efficient and lasting loss of N-WASP protein in the epidermis (Fig. 1A). N-WASP mutant mice showed a delayed growth (supplementary material Fig. S1), but no increased lethality.

To assess whether loss of N-WASP leads to aberrant keratinocyte differentiation, we performed immunofluorescent stainings for a panel of marker proteins of interfollicular epidermis and hair follicles. In the interfollicular epidermis, K14 (basal and lower suprabasal cells), K10 (suprabasal cells), and loricrin (terminally differentiating cells) were normally distributed in back skin of 9-day-old N-WASP mutant mice (Fig. 1B). K6, a marker for hyperproliferative keratinocytes, was not detectable in the interfollicular epidermis (Fig. 1B). Expression of α6 integrin (a subunit of the basement membrane receptor α6β4 integrin) and deposition of the basement-membrane component laminin 332 was similar in control and N-WASP mutant mice (Fig. 1B). No obvious alteration was found in the distribution of E-cadherin and F-actin (Fig. 1B).

**Fig. 1. Normal epidermal differentiation and maintenance in N-WASP fl/fl K5 mice.** (**A**) Western blot for N-WASP on epidermal lysates from 5-day-old and 1-year-old control (con) and N-WASP fl/fl K5 Cre (ko) mice. (**B**) Sections of back skin of 9-day-old control ko mice were analyzed by histochemical staining and immunofluorescence. Top panel: staining with HE. Below, from top to bottom: LN332, K14, K10, loricrin and K6 (all in red with counterstaining for α6 integrin in green to indicate the dermal-epidermal junction), E-cadherin (red) and F-actin (green). Nuclear DNA was visualized using Draq5 or DAPI (blue). Scale bar: 50 μm.

Journal of Cell Science

Furthermore, proliferation of basal keratinocytes in the interfollicular epidermis was not significantly altered in the absence of N-WASP at 9 days, 2, 3 and 7 weeks of age, as measured by BrdU incorporation (supplementary material Table S1). Finally, transmission electron microscopy examination of 2-week-old mice revealed no major structural alterations in interfollicular epidermis in the absence of N-WASP compared with controls. N-WASP-deficient mice displayed normal keratinocytes and were able to form desmosomes, hemidesmosomes and structured basement membrane of normal appearance, although subtle differences cannot be excluded (supplementary material Fig. S2).

### N-WASP fl/fl K5 mice develop cyclic alopecia and abnormal hair-follicle cycling

In the absence of N-WASP, development of hair follicles, which continues in mice during early postnatal life until the initiation of hair-follicle cycling and is often misinterpreted as 'first hair cycle' (Paus et al., 1999), was significantly delayed during the first 2 weeks after birth, lagging behind by one or two morphogenesis stages (Fig. 2A and supplementary material Fig. S3A). After initiation of hair-follicle cycling, mutant mice lost their hair rapidly, resulting in a nearly complete loss of hairs at 5-6 weeks of age (Fig. 2B). This baldness (alopecia), however, was not permanent because at 7 weeks N-WASP-deficient mice had regained long, pigmented, terminal hair shafts in most skin regions (Fig. 2B, Fig. 3B). Subsequently, N-WASP mutant mice lost and regained fur continually, resulting in an unusual, cyclic-alopecia phenotype similar to the one described for *Msx2* knockout mice (Ma et al., 2003). We noted that different skin regions, which were varying in their outlines from mouse to mouse, seemed to cycle synchronously, but independently from each other (Fig. 2B; arrows and arrowheads). This phenomenon had been described earlier for other mouse strains (Ma et al., 2003; Plikus et al., 2008) and probably reflects an impact of N-WASP deletion on the intra- and/or extrafollicular oscillator systems that drive wave patterning and determine formation of hair domains during murine hair-follicle cycling (Plikus et al., 2008).

Although N-WASP-deficient mice never showed a normal fur coat again, regrowth of hair in isolated domains could still be observed even in 6-month-old mice (data not shown). The reduced fur of N-WASP-deficient mice possibly explains their delayed growth as being due to a higher energy consumption. No significant difference was found in the total number of hair follicles per length of epidermis between control and mutant mice between the ages of 5 days and 1 year (Fig. 3A), indicating that the hair loss seen in N-WASP mutants does not result from a loss of hair follicles as such.

### No obvious defect in hair-follicle keratinocyte differentiation in the absence of N-WASP, but abnormal widening of the hair canal

To investigate whether the hair loss corresponds to changes in the differentiation of hair-follicle keratinocytes, we performed immunohistological staining for marker keratins that are expressed in defined compartments of the hair-follicle epithelium [i.e. in the companion layer (K75, K6), the inner root sheet (IRS) layers Henle, Huxley and cuticle (K71) or the IRS-cuticle (K73), the hair cuticle (K82) and the hair cortex (K33, K34) (Langbein and Schweizer, 2005)]. Furthermore, we have also looked in the medulla for these keratins. Yet, we could not detect significant immunoreactivity differences between control and N-WASP-deficient hair follicles of 9-day-old mice (Fig. 4A; supplementary material Fig. S3B). No expression of interfollicular markers (K10, loricrin) was found in the hair follicles of N-WASP mutant mice (data not shown). This differed from previously reported mice lacking the N-WASP activator Cdc42 in keratinocytes, which showed loss of hair-follicle-specific keratins and gain of proteins normally restricted to the interfollicular epidermis in hair follicles (Wu et al., 2006c). As in the epidermis, we could not detect any alteration in the staining for E-cadherin and F-actin (Fig. 4A).

Epithelial-mesenchymal interactions between hair-follicle keratinocytes and inductive fibroblasts of the follicular dermal papilla are important for hair-follicle cycling (Stenn and Paus, 2001). However, demarcation of dermal papilla fibroblasts by versican immunostaining or alkaline phosphatase activity [both of which are correlated with the inductive potential of this specialized fibroblast

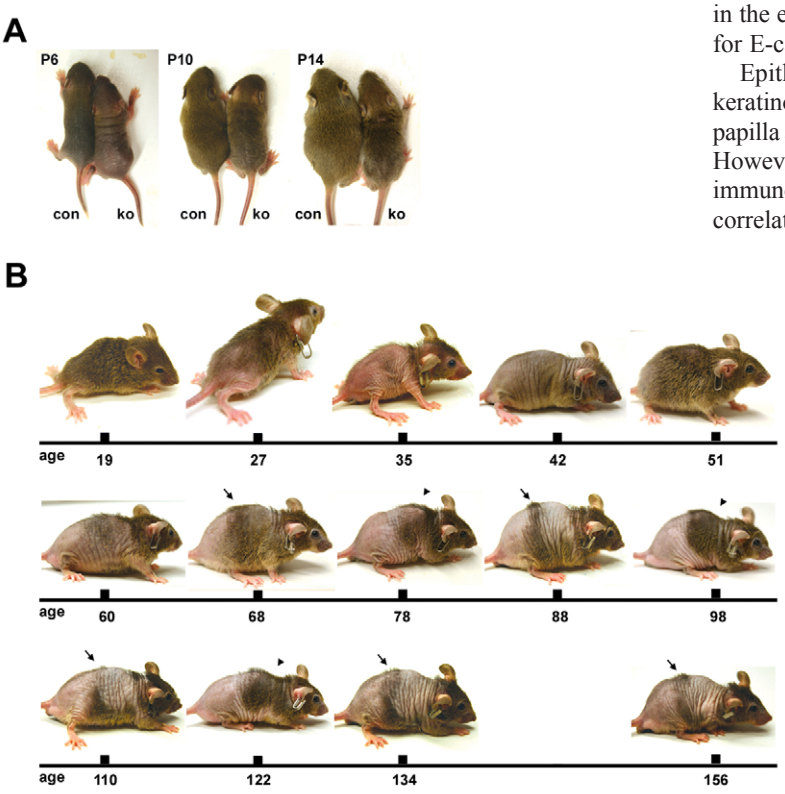


**Fig. 2. Cyclic alopecia in mice with a keratinocyte-restricted deletion of the N-WASP gene.** (**A**) Photographs of a N-WASP mutant mouse (ko) at the indicated ages, alongside a littermate control (con). (**B**) Photographs of a N-WASP fl/fl K5 Cre mouse taken at the indicated ages. Independently cycling regions are indicated by arrows and arrowheads.

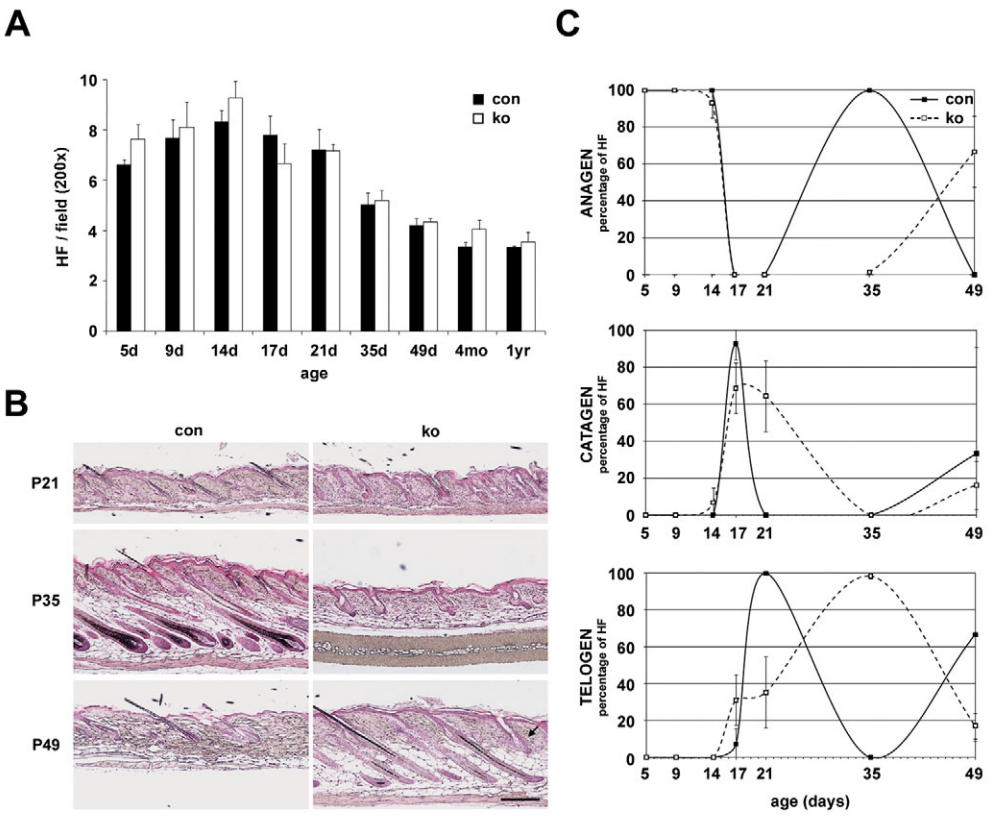


**Fig. 3. Hair-cycle abnormalities in N-WASP mutant mice.** (**A**) HE-stained paraffin sections of control (con) and N-WASP fl/fl K5 Cre (ko) mice were investigated at 200-fold magnification and the number of hair canals transecting the epidermis per field was counted for a minimum of 20 fields per time point (means ± s.d., $n \geq 3$). (**B**) HE-stained sections of back skin at 21, 35 and 49 days. Note telogen follicle in ko at 49 days (arrow). Scale bar: 200 µm. (**C**) More detailed analysis of the hair cycle was performed. Percentages of hair follicles (HF) in anagen (top), catagen (middle) and telogen (bottom) were plotted for ages between 5 and 49 days. More than 40 hair follicles were investigated per time point (means ± s.d., $n \geq 3$).

population (Stenn and Paus, 2001)] did not reveal any overt differences in anagen hair follicles of control and mutant mice (supplementary material Fig. S4A).

Because hair shafts are not normally shed during the first rounds of hair-follicle cycling in mice, the alopecia phenotype observed here suggested an underlying structural abnormality that weakened the anchorage of hair shafts in their epithelial mooring, such as widening of the hair canal. To investigate, therefore, whether such an alteration could contribute to the alopecia phenotype, we analyzed the skin at 3 weeks, i.e. the age at which hair loss started to become apparent. In control mice, all club hairs observed were firmly embedded in the surrounding tissue. However, in mutant mice we found that a substantial number of the observed club hairs (67±4%; $n$=3) were only loosely surrounded by a markedly distended hair canal, often accompanied by aberrant club hair morphology (Fig. 4B). Thus, widening of the follicular canal, which might also promote both excessive passive and active shedding of the hair shaft (exogen) (Stenn and Paus, 2001), is probably the reason for the hair loss. To assess whether increased keratinocyte death might contribute to the abnormal widening of the hair canal in N-WASP mutant mice, we stained skin sections of 17-day-old mice for the apoptotic marker cleaved caspase-3. Indeed, N-WASP mutant hair follicles showed a twofold increase in caspase-3-positive cells per hair follicle, suggesting that loss of N-WASP promotes apoptosis of hair-follicle keratinocytes during catagen, thus contributing to the abnormal widening of the hair canal (Fig. 4C).

Taken together, these data show that K5-targeted loss of N-WASP does not block or distort keratinocyte differentiation in either the interfollicular epidermis or the hair-follicle epithelium. However, it facilitates apoptosis-driven hair-follicle involution and induces changes in the structure of hair follicles that compromise anchorage of the hair shaft in the hair canal, resulting in alopecia.

### Defective hair cycle in N-WASP mutant mice

In the light of the normal total number of hair follicles in N-WASP fl/fl K5 mice (Fig. 3A), the cyclic and domain-restricted nature of the observed hair-loss phenotype (see above) also suggested the possibility of a profound underlying abnormality in normal patterns of murine hair-follicle cycling. To test this hypothesis, we investigated whether absence of N-WASP leads to defective timing of the hair cycle.

Indeed, N-WASP-deficient mice displayed a strongly impaired hair cycle (Fig. 3B). At 3 weeks, all hair follicles in control mice were in telogen, as opposed to the hair follicles of mutant mice, all of which were in late catagen or telogen. At 5 weeks, only hair follicles of control mice were in full anagen, whereas nearly all hair follicles of mutant mice were still in telogen. At 7 weeks, the opposite was seen. Most hair follicles of control mice were in the resting phase (telogen), whereas the majority of hair follicles in mutant mice were in anagen. More detailed analysis of the hair-cycling phenotype revealed that, postnatally, the end of morphogenesis stage 8 and entry into hair-follicle cycling by the first induction of catagen (Müller-Röver et al., 2001; Paus et al., 1999) were almost synchronous in control and mutant mice (Fig. 3C). Exit from the first resting phase, however, was severely delayed in the absence of N-WASP. Furthermore, in contrast to wild-type mice, initiation of the first postnatal anagen did not occur synchronously in all mutant hair follicles, as indicated by the highly abnormal presence of full-length anagen follicles (75%) side-by-side with catagen (10%) or telogen (15%) hair follicles at 7 weeks of age (Fig. 3C). These results reveal a major

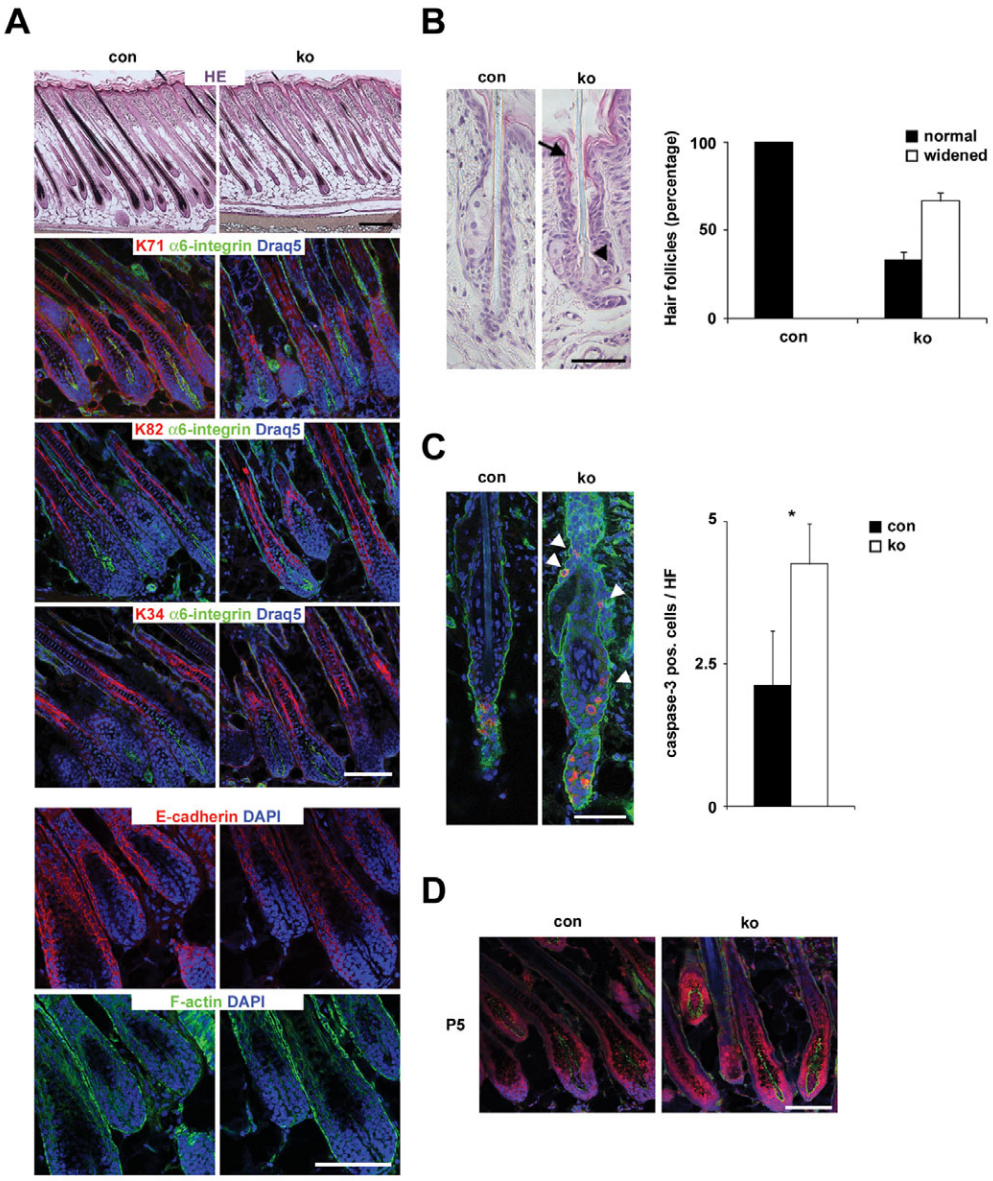


**Fig. 4. Normal differentiation of the hair-follicle epithelia in the absence of N-WASP but abnormal hair canal widening.** (**A**) Sections of back skin of 9-day-old control (con) and N-WASP fl/fl K5 Cre (ko) mice were analyzed by histochemical staining and immunofluorescence. From top to bottom: HE staining. Scale bar: 200 μm. K71, K82 and K34 [all in red with counterstaining for α6 integrin to indicate the dermal-epidermal junction (green)], E-cadherin (red) and F-actin (green). Nuclear DNA was stained with Draq5 or DAPI (blue). Scale bars: 100 μm. (**B**) HE-stained sections of back skin of 3-week-old control and ko mice. Control hair follicles show normal club hairs closely surrounded by hair follicle tissues, ko hair follicles frequently have a widened hair canal (arrow) and malformed club hairs (arrowhead). Scale bar: 50 μm. Graph shows percentage of club hairs found in normal or widened hair canals for both control and ko mice (means ± s.d., $n$=3). (**C**) Back skin sections of 17-day-old control and ko mice were stained for cleaved caspase-3 (red). α6 integrin staining (green) indicates the dermal-epidermal junction; nuclear DNA was stained with DAPI (blue). Scale bar: 50 μm. Note the position of apoptotic cells in ko (arrowheads). Graph shows average amount of cleaved caspase-3-positive cells found per hair follicle (HF). Asterisk indicates significant changes, $P$<0.05, means ± s.d., $n$=3. (**D**) Cryosections from the back skin of 5-day-old control and ko mice were analyzed by immunofluorescence for the presence of Msx2 (red). Counterstaining for α6 integrin was used to indicate the dermal-epidermal junction (green); nuclear DNA was visualized using DAPI (blue). Scale bar: 100 μm.

disturbance of hair-follicle cycling by keratinocyte-targeted deletion of N-WASP.

### No change in Msx2 expression

A cyclic-alopecia phenotype in mice has been previously described in mice lacking the transcription factor Msx2 (Ma et al., 2003). These mice showed a premature and prolonged catagen, and defective hair shaft differentiation. In the absence of N-WASP, however, immunofluorescent staining for Msx2 was indistinguishable from controls in skin of 5-day-old mice (Fig. 4D). Furthermore, expression of *Msx2* mRNA was not altered in N-WASP-deficient primary keratinocytes as determined by microarray gene expression analysis (1.1-fold change, $n$=3). The normal expression of Msx2 and the slightly different phenotype of the *Msx2* mutant mice suggest that N-WASP acts on the intra- and/or extrafollicular oscillator systems that underlie the 'hair cycle clock' (Paus and Foitzik, 2004; Plikus et al., 2008) via a different pathway to that of Msx2.

### Normal Erk activation in N-WASP-deficient hair follicles

The delay in hair-follicle morphogenesis and anagen re-entry in N-WASP mutant mice suggested that N-WASP function is important for keratinocyte proliferation in hair follicles. We therefore hypothesized that the delayed anagen onset in N-WASP mutant mice might be due to a reduction in proliferative signals. Because many proliferative signals result in an activation of extracellular-signal-regulated kinase (Erk), we investigated the amount of active, phosphorylated Erk (Erk-*P*) by immunofluorescent staining at different time points.

At 5 days, Erk-*P* was similarly detectable both in control and mutant hair follicles. At 5 weeks, however, Erk-*P* was nearly exclusively detected in control hair follicles. By contrast, Erk-*P* was found in 7-week-old mice in the majority of mutant hair follicles, but not in control hair follicles (Fig. 5A). Erk activation therefore correlated well with the anagen phase of the hair cycle, but was not detectably different in control and mutant hair follicles of the same hair-cycle stage.

Journal of Cell Science

In order to detect more subtle differences in Erk phosphorylation, we conducted western blot analysis and quantified the results. In all lysates from mice older than 5 weeks, Erk activation was reduced in N-WASP-deficient mice (data not shown). However, if Erk-*P* is particularly high in anagen hair follicles, as the immunostaining results implied, this difference could be caused by a reduced percentage of anagen hair follicles in N-WASP mutant mice at all these late time points. To avoid this problem, we assessed lysates from 3-week-old mice, because at this stage there are no hair follicles in anagen in either control or mutant mice. No significant difference was detected in Erk-*P* levels between control and mutant mice at this time point (Fig. 5B). These data suggest that the impaired exit from the resting phase of the hair cycle in N-WASP mutants is not due to a reduced Erk activation.

### Increased p21CIP expression in the absence of N-WASP

Because there was no obvious change in Erk-activating proliferative signals, we next assessed whether loss of N-WASP might cause an increase of antiproliferative signals. To test this, we checked for expression of the cell-cycle inhibitor p21CIP, because it was previously shown in mice with a keratinocyte-specific loss of calcineurin B1 that decreased p21CIP levels correlate with premature anagen onset (Mammucari et al., 2005). Indeed, western blot analysis of epidermal lysates of 3-week-old mice revealed a significant increase of p21CIP expression in N-WASP mutant mice (Fig. 6A). Quantification of the staining intensity of immunofluorescent analysis confirmed increased levels of nuclear p21CIP, both in hair follicles and in the interfollicular epidermis of 3-week-old N-WASP mutant mice (Fig. 6B).

To investigate whether the increased expression of p21CIP corresponds to a reduced proliferation of hair follicles, we performed a BrdU-incorporation assay. Proliferation of hair matrix cells was not altered in 9-day-, 2-week- or 3-week-old N-WASP-deficient mice (supplementary material Table S1), suggesting that N-WASP facilitates the initiation of hair-follicle growth, but is not required for proliferation of hair follicle cells. At 7 weeks of age, *N-WASP*-null hair follicles showed higher, but also much more variable proliferation than control hair follicles, because at that time nearly all control hair follicles were in resting phase, whereas most mutant hair follicles were in anagen (see Fig. 3C).

These data show that loss of N-WASP increases p21CIP expression in keratinocytes in hair-follicle resting phase, correlating with a delayed entry into anagen of the mutant hair follicles.

### Increased TGFβ signaling in vivo in the absence of N-WASP

In keratinocytes, Notch signaling controls p21CIP expression in vitro and in vivo (Mammucari et al., 2005; Rangarajan et al., 2001). Other pathways known to regulate p21CIP expression are bone morphogenetic protein (BMP) and transforming growth factor β (TGFβ) signaling (Pardali et al., 2005). All three pathways are now recognized as key regulators of hair-follicle cycling and wave-pattern formation (Plikus et al., 2008; Stenn and Paus, 2001).

To determine which signaling mechanism contributes to the increased expression of p21CIP in N-WASP-deficient epidermis, we assessed the activation of Notch, BMP and TGFβ signaling.

Western blot analysis of epidermal lysates of 3-week-old control and mutant mice showed decreased expression of the Notch target HES-1 in the absence of N-WASP, suggesting decreased Notch signaling (Fig. 7). Because this should result in reduced p21CIP expression (Mammucari et al., 2005; Rangarajan et al., 2001), this alteration cannot explain the increased amounts of p21CIP in N-WASP mutants. BMP signaling was not significantly changed in the absence of N-WASP, because phosphorylation of Smad1/5/8 was similar in control and N-WASP mutant mice (Fig. 7), not supporting a role of BMP signaling downstream of N-WASP. The TGFβ signaling molecule Smad2, however, showed significantly increased phosphorylation in N-WASP mutant animals, indicating enhanced TGFβ signaling (Fig. 7). Increased TGFβ signaling in N-WASP mutant mice was further supported by the elevated levels of the negative feedback regulator Smad7 (Fig. 7). However, we could not detect increased expression of the gene encoding the cell-cycle inhibitor p15INK4B, which is a known TGFβ target gene in keratinocytes in vitro (Fig. 7). Whereas expression of the TGFβRI was increased in the absence of N-WASP, TGFβRII expression was decreased (Fig. 7), indicating a complex regulation of TGFβ signaling by N-WASP in vivo. TGFβ expression was not altered in

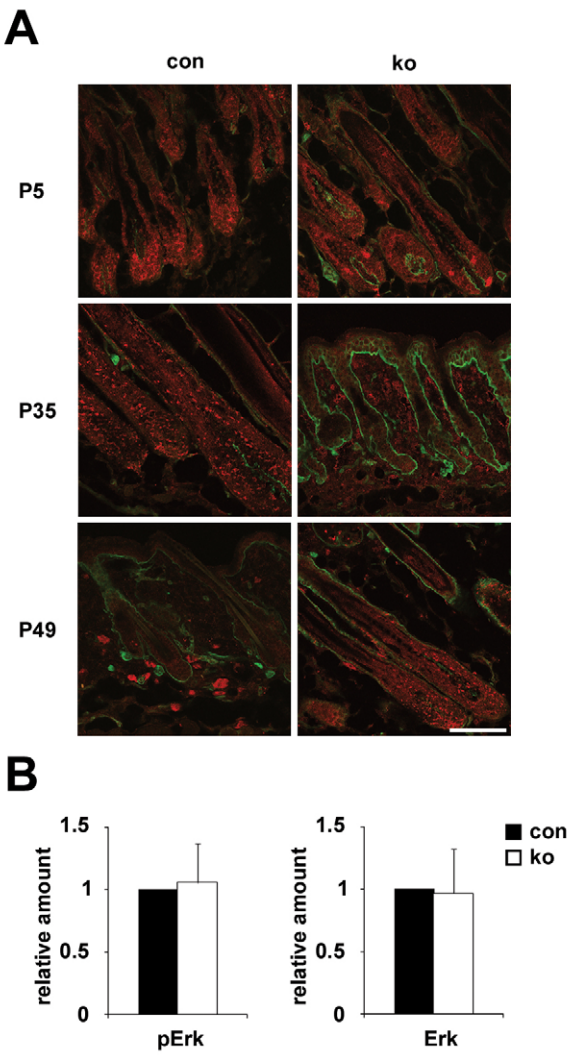


**Fig. 5. Normal Erk activation in epidermis and hair follicles of N-WASP mutant mice.** (**A**) Cryosections of control (con) and N-WASP fl/fl K5 Cre (ko) back skin were stained for the presence of phosphorylated Erk (pErk, red), with counterstaining for α6 integrin to indicate the dermal-epidermal junction (green). Scale bar: 100 μm. (**B**) Western blot analysis of epidermal lysates of 3-week-old control and ko mice. Bar graphs indicate relative expression level compared with control mice (means ± s.d., *n*=3).

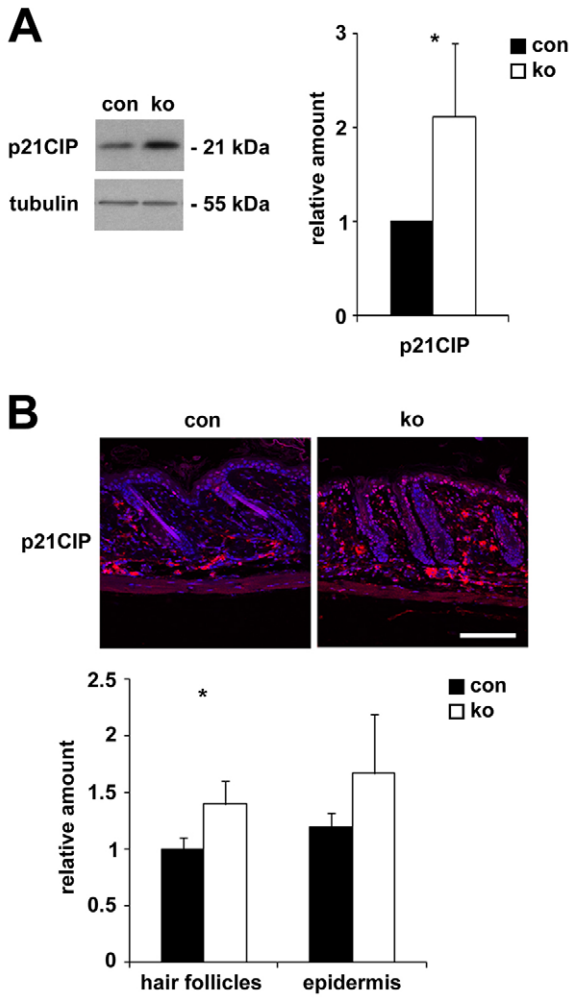


**Fig. 6. Increased p21CIP expression in the absence of N-WASP.** (**A**) Western blot analysis of epidermal lysates of 3-week-old control (con) and N-WASP fl/fl K5 Cre (ko) mice. Representative blot and bar graph indicating relative expression levels compared with control mice. **P*<0.001, means ± s.d., *n*=15. (**B**) p21CIP (red) staining on back skin sections of 3-week-old control and ko mice. Nuclei stained with DAPI (blue). **P*<0.05, means ± s.d., *n*=3.

N-WASP-deficient epidermal lysates (Fig. 7) and showed similar distribution in control and mutant skin, as tested by immunofluorescent staining with an antibody recognizing TGFβ1, TGFβ2 and TGFβ3 (supplementary material Fig. S4B).

These findings indicate that N-WASP regulates TGFβ receptor signaling in keratinocytes in vivo and suggest that the increase in p21CIP might be downstream of increased TGFβ receptor activation.

### Growth defect of primary *N-WASP*-null keratinocytes in vitro

To test whether the delayed anagen onset in vivo corresponds to altered growth behaviour of *N-WASP*-null keratinocytes under hyperproliferative conditions in vitro, we investigated the growth of primary *N-WASP*-null keratinocytes in low calcium medium, which promotes keratinocyte proliferation in vitro. *N-WASP*-null keratinocytes showed a normal morphology and actin cytoskeleton, including formation of focal adhesions (supplementary material Fig. S5A). However, N-WASP-deficient keratinocytes grew slower than control keratinocytes, and displayed a significant increase of cells in the G1 phase, indicating a defect in G1-S transition (Fig. 8A,B). This growth defect was not caused by impaired adhesion, increased apoptosis or premature differentiation of *N-WASP*-null keratinocytes (supplementary material Fig. S5B,C).

These results indicate that primary *N-WASP*-null keratinocytes have an impaired proliferation in vitro.

### Differential keratinocyte gene expression in the absence of N-WASP

To identify changes in gene expression corresponding to the growth defect observed in keratinocytes in vitro, we performed a microarray analysis of primary keratinocytes isolated from 3-week-old control and mutant mice after 6 days in culture (supplementary material Table S2). Functional annotation of the 31 genes upregulated more than 2.5-fold by the DAVID program (Dennis et al., 2003) revealed larger groups for the categories alternative splicing (35%), signal (35%), phosphoprotein (26%), glycoprotein (24%), secreted (21%), membrane (18%) and cytoplasm (18%). WASP was not upregulated in N-WASP mutant keratinocytes, suggesting that the phenotype is not affected by compensatory upregulation of a functionally related molecule.

Most strikingly, we observed a 2.5-fold upregulation of the gene encoding the cell-cycle inhibitor p15INK4B (*Cdkn2b*), which is a well-known target gene of TGFβ signaling in human keratinocytes (Reynisdóttir et al., 1995). p21CIP was only slightly upregulated on the transcriptional level (1.2-fold). Among the 31 genes significantly upregulated more than 2.5-fold, we found nine genes previously described to be regulated by TGFβ, three genes (all of them overlapping with TGFβ target genes) described to be regulated by BMP, but no genes known to be regulated by Notch (Fig. 8C). Furthermore, we observed 1.5-fold upregulation of Smad7 and 1.8-fold downregulation of TGFβ-RIII, which are indicative of negative feedback regulation of the TGFβ pathway (Hempel et al., 2008; Ten Dijke et al., 2002). In contrast to mice lacking the N-WASP activator Cdc42 in keratinocytes (Wu et al., 2006c), we did not find any indication for increased Wnt activity in the list of strongly upregulated genes. Only three genes were significantly downregulated more than 2.5-fold (see supplementary material Table S2).

qRT-PCR of the RNA samples used for microcarray and 3-6 additional samples confirmed the increased expression of the TGFβ target genes encoding p15INK4B (Fig. 9B), Fn1 (3.58±1.72 fold; *n*=6), CXCL12 (2.07±1.15 fold; *n*=6), and TNC (1.80±1.02; *n*=6) in N-WASP knockout (ko) cells, and showed a trend towards increased expression of Chn2 (1.31±0.8 fold; *n*=6), whereas Col8A1 (0.90±0.31; *n*=6) was not found to be upregulated.

Western blot analysis of primary keratinocytes suggested a slight upregulation of p21CIP protein and pSmad2 in the absence of N-WASP. However, these differences were not significant due to very high inter-individual variations between mice (supplementary material Fig. S5D). Therefore, although the expression of various TGFβ target genes reflected increased TGFβ signaling in *N-WASP*-null keratinocytes, the protein levels of the TGFβ target p21CIP and the phosphorylation level of the TGFβ effector Smad2 varied. This is most probably due to the well-recognized negative feedback regulation by Smad7 (Ten Dijke et al., 2002), which was detected in the gene expression array. Furthermore, p21CIP expression in keratinocytes in vitro was reported to be strongly upregulated in response to increasing cell density (Cho et al., 2008). Due to the severe growth defect of N-WASP keratinocytes in vitro, the cell density for

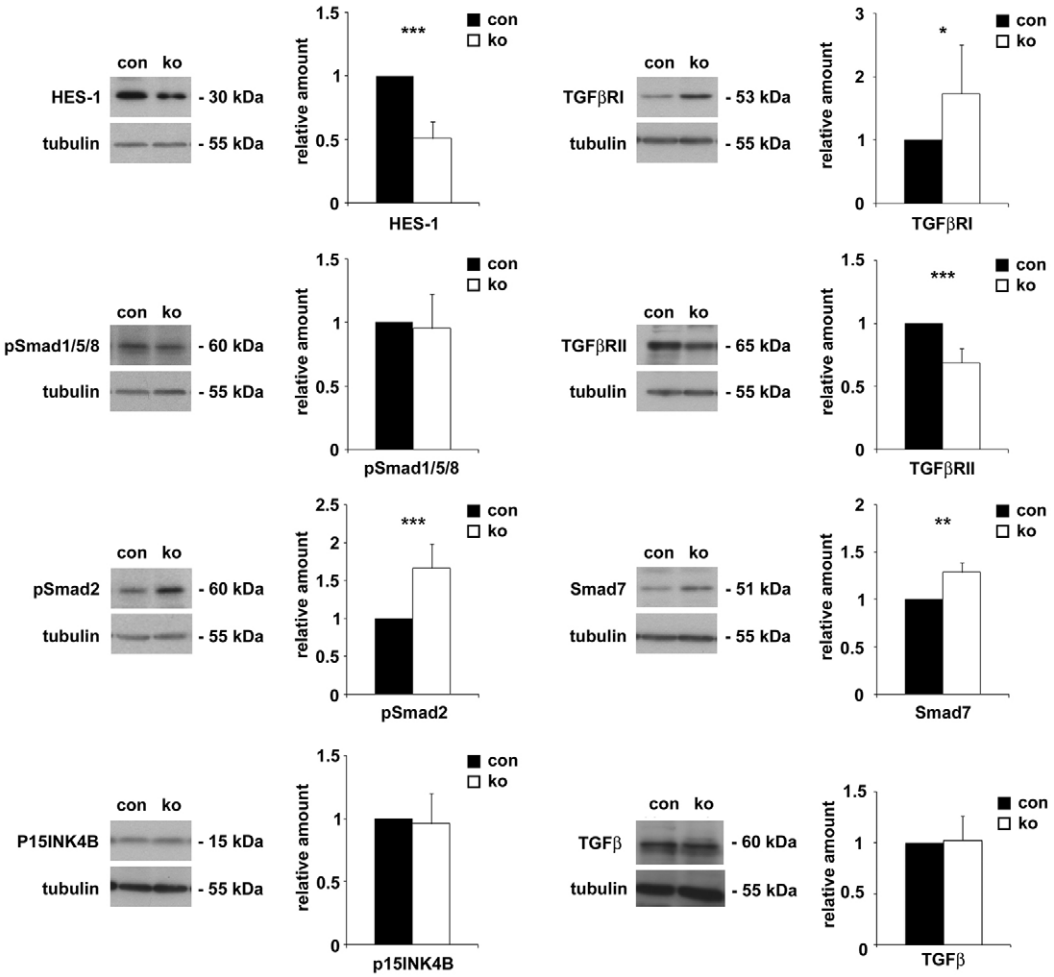


**Fig. 7. Increased TGFβ signaling in N-WASP mutant mice.** Western blot analysis on epidermal lysates of 3-week-old control (con) and N-WASP fl/fl K5 Cre (ko) mice. Representative blots and bar graphs indicate relative expression levels compared with control mice (means ± s.d.). ***$P$<0.001, **$P$<0.01, *$P$<0.05; HES-1 and pSmad158, $n$=7; pSmad2, $n$=12; P15INK4B, $n$=6; TGFβRI, $n$=9; TGFβRII, $n$=5; Smad7, $n$=3; TGFβ, $n$=3.

control and mutant keratinocytes was rather different throughout the experiments and the higher density of control cells could have increased their p21CIP expression. This effect might mask a relatively small N-WASP-dependent effect on p21CIP expression.

Microarray analysis did not detect increased expression of TGFβ1, TGFβ2, TGFβ3, TGFβRI or TGFβRII in N-WASP-deficient keratinocytes (data not shown). Changes in TGFβRI and TGFβRII protein amounts as observed in epidermal lysates of *N-WASP*-null mice (Fig. 7) are therefore most probably caused by altered receptor turnover. Thus, the impaired proliferation of *N-WASP*-null keratinocytes in vitro correlated best with increased TGFβ signaling and increased expression of the cell-cycle inhibitor p15INK4B.

### Inhibition of TGFβ signaling rescues the proliferation defect of primary *N-WASP*-null keratinocytes

Because the above findings suggested that increased TGFβ signaling is responsible for the impaired proliferation of *N-WASP*-null keratinocytes in vitro, we tried to rescue their growth defect by inhibiting TGFβ signaling. Primary keratinocytes were treated with different amounts of TGFβ RI kinase inhibitor II for 5 days, and the cell growth during the last 4 days of treatment was investigated. At inhibitor concentrations of less than 10 ng/ml, which are not sufficient to effectively block TGFβ signaling, growth of N-WASP-deficient keratinocytes was significantly reduced (Fig. 9A). At higher inhibitor concentrations, proliferation of control and mutant cells was not significantly different, indicating that inhibition of TGFβ signaling rescues the growth defect observed in *N-WASP*-null keratinocytes. Both in control and mutant cells, inhibitor treatment increased keratinocyte proliferation.

We then used qRT-PCR to test whether the TGFβRI inhibitor reduced the overexpression of the cell-cycle inhibitor p15INK4B to levels similar to inhibitor-treated control cells. Indeed, treatment with the TGFβRI inhibitor significantly decreased p15INK4B expression in control and *N-WASP*-null keratinocytes (Fig. 9B). There was no significant difference between control and mutant cells following inhibitor treatment.

This rescue experiment indicated that the reduced proliferation of primary *N-WASP*-null keratinocytes in vitro is mediated by TGFβR-dependent expression of the cell-cycle inhibitor p15INK4B.

### *N-WASP*-null epidermis shows normal wound healing

Under physiological conditions in vivo, *N-WASP*-null keratinocytes showed normal proliferation. In hyperproliferative culture

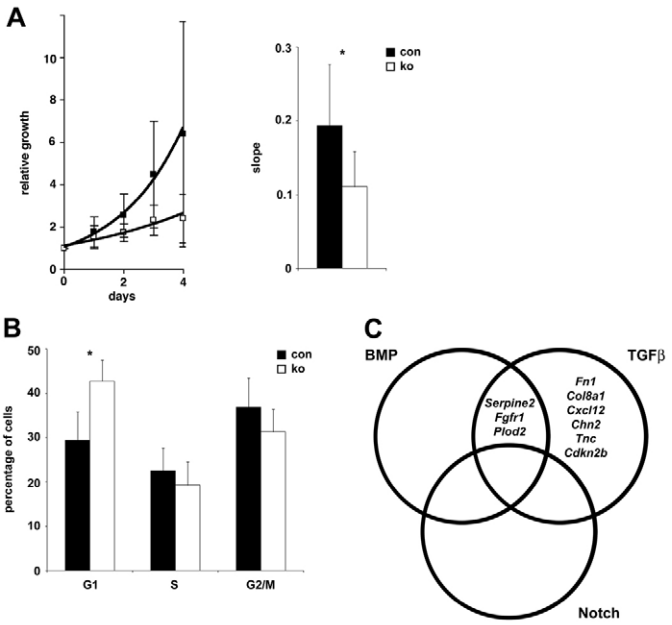


**Fig. 8. In vitro growth defect of *N-WASP*-null keratinocytes.** Primary keratinocytes from N-WASP fl/fl K5 Cre (ko) and control (con) mice were isolated and cultured under low calcium conditions. (**A**) Growth curve with exponential curve fits. Bar graph shows the slope of the linear regression line through the semi-logarithmically plotted growth over 4 days. **P*<0.05, means ± s.d., *n*=11. (**B**) Cell cycle was investigated by FACS analysis. Bar graph shows the percentages of cells in G1, S and G2-M phases. **P*<0.001; means ± s.d.; con, *n*=9; ko, *n*=7. (**C**) Microarray analysis of cultured keratinocytes uncovered 31 genes that were significantly upregulated more than 2.5-fold in N-WASP mutant cells compared with control cells. The diagram shows those genes that have been previously described to be regulated by the BMP, TGFβ or Notch pathways.

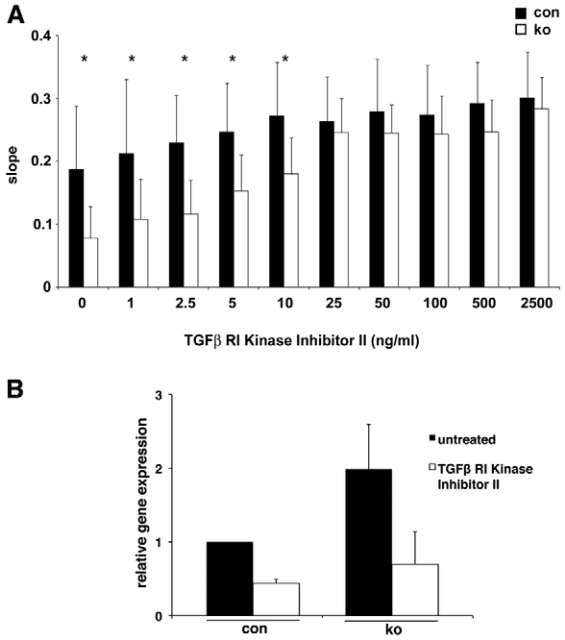


**Fig. 9. Rescue of the in vitro growth defect of *N-WASP*-null keratinocytes by inhibition of TGFβ, corresponding to normalized p15INK4B expression.** (**A**) Primary keratinocytes were treated with a TGFβ receptor inhibitor (TGFβ RI kinase inhibitor II) at concentrations ranging from 0 to 2500 ng/ml. Bar graph shows the slope of the linear regression line through the semi-logarithmically plotted growth over 4 days of culture in medium containing inhibitor. **P*<0.05, means ± s.d., *n*=8. (**B**) Primary keratinocytes treated with or without 50 ng/ml TGFβ RI kinase inhibitor II for 3 days were analyzed for expression of p15INK4B by qRT-PCR. Untreated *N-WASP*-null keratinocytes showed significantly increased p15INK4B expression compared with control. Treatment with the TGFβ receptor inhibitor significantly reduced (*P*<0.05; untreated cells, *n*=9; treated cells, *n*=3) p15INK4B in control and mutant cells to levels that were not significantly different from each other.

conditions in vitro, however, N-WASP-deficient keratinocytes displayed a severe TGFβ-dependent growth defect. It therefore seems possible that *N-WASP*-null epidermis might show defective growth in hyperproliferative conditions in vivo. For that reason, we tested whether wounding-induced hyperproliferation is impaired in N-WASP mutant mice.

Full-thickness wounds were inflicted to the back of control and N-WASP ko mice, and after 3 days the wound closure and BrdU incorporation were determined. No significant differences were found in wound closure [control, 1±0.41 (four wounds, three mice); ko, 1.09±0.08 (six wounds, three mice)] and wound-induced hyperproliferation [percentage of BrdU+ keratinocytes in hyperproliferative epidermis: control, 0.27±0.1% (four wounds, three mice); ko, 0.26±0.08% (six wounds, three mice)], indicating that N-WASP is not required for keratinocyte migration during wound healing and that wound-induced growth signaling is not strongly affected by the loss of N-WASP.

### Altered TGFβ signaling of *N-WASP*-null keratinocytes is dependent on gene deletion in vivo

The previous experiments indicated that loss of N-WASP in keratinocytes increases TGFβ signaling in vivo. To assess whether this phenotype is dependent on gene deletion in vivo, we isolated primary keratinocytes from N-WASP fl/fl mice, induced gene deletion in vitro by transfection of a Cre and GFP co-expressing plasmid, and investigated TGFβ signaling and cell proliferation in vitro. FACS-sorted GFP+ cells showed a virtually complete loss of N-WASP protein (data not shown) only 3 days after transfection. However, analysis of sorted GFP+ cells 3-6 days after transfection revealed no obvious increase in TGFβ signaling (Fig. 10A). Whereas pSmad2, p21CIP and p15INK4B were slightly increased at day 3, there was no increase of p21CIP or p15INK4B detectable at days 4-6. Moreover, Smad7 expression was decreased after 4-6 days, not supporting an increased TGFβ signaling. No significant alteration was found in TGFβRI levels.

Measuring the percentage of GFP+ cells among keratinocytes of N-WASP fl/+ or N-WASP fl/fl mice transfected in vitro with GFP and Cre or with GFP alone, indicated a toxic effect of Cre expression in keratinocytes, but no growth inhibition of *N-WASP*-null keratinocytes, when the gene deletion occurred in vitro (Fig. 10B).

These data suggest that the establishment of the effect of N-WASP on TGFβ signaling is either dependent on the interaction of *N-WASP*-null keratinocytes with other cell types in vivo, or on the growth conditions in vivo (three dimensions, extracellular matrix, growth factors), which are not sufficiently mimicked in vitro.

Journal of Cell Science

Journal of Cell Science

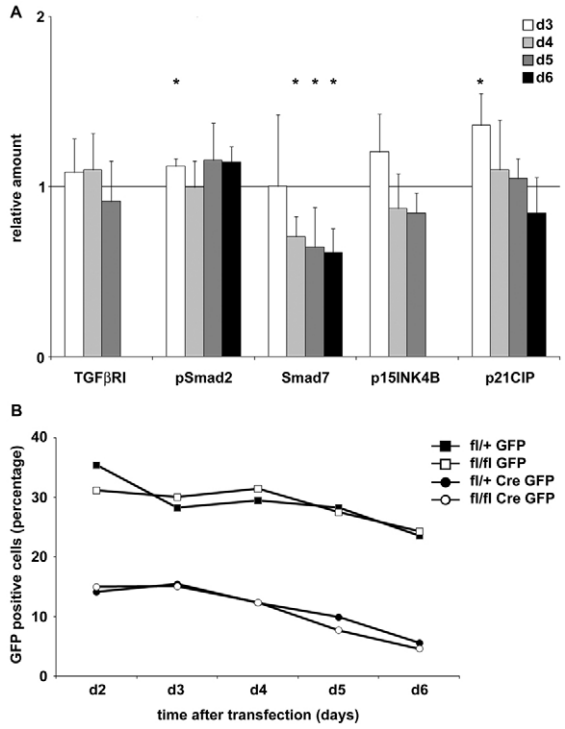


**Fig. 10. Induction of N-WASP gene deletion in vitro does not strongly alter TGFβ signaling and cell growth.** (**A**) Western blot analysis on lysates of sorted GFP and Cre-GFP transfected N-WASP fl/fl keratinocytes. Bar graphs show relative expressions levels of proteins in N-WASP fl/fl Cre-GFP cells compared with N-WASP fl/fl GFP cells on the indicated times after transfection. **P*<0.05, means ± s.d., *n*≥3. (**B**) N-WASP fl/fl and N-WASP fl/+ cells were transfected with GFP or Cre-GFP constructs and analyzed by FACS. Graph shows the percentages of GFP and Cre-GFP positive cells at the indicated times after transfection (*n*=2).

## Discussion

This study identifies the actin nucleation regulator N-WASP as a novel regulator of hair-follicle cycling, and demonstrates that N-WASP is required for timely telogen-anagen transition. Several factors, including Wnts, KGF, HGF and TGFα, have previously been shown to affect the telogen-anagen transition (Paus and Foitzik, 2004). Our current data now suggest that N-WASP regulates anagen re-entry primarily by controlling TGFβ signaling, which inhibits anagen onset via increased expression of the cell-cycle inhibitor p21CIP and inhibits keratinocyte proliferation in vitro by increased expression of the cell-cycle inhibitor p15INK4B. Because hair-follicle cycling is an important model for organ regeneration and cyclic transformation, our study reveals an important, previously unknown function of N-WASP in epithelial biology, and indicates the regulation of TGFβ signaling as a major pathway downstream of this actin nucleation regulator in vivo.

Several observations demonstrate the regulation of TGFβ signaling by N-WASP. First, phosphorylation of Smad2, which is directly phosphorylated by the activated TGFβRII, is increased in N-WASP-deficient epidermis. Second, expression of nuclear p21CIP, a known TGFβ effector, is increased in *N-WASP*-null keratinocytes in vivo, whereas the p21CIP-inducing pathways Notch and BMP show either decreased or unaltered activity. Third, primary *N-WASP*-null keratinocytes display increased expression of several TGFβ target genes, including p15INK4B, whereas no similar increase in Notch or BMP target gene expression was observed. Fourth, increased expression of Smad7 and decreased expression of TGFβRIII in N-WASP-deficient keratinocytes indicate negative feedback regulation of TGFβ signaling, thus implying a preceding increase in TGFβ signaling. Fifth, N-WASP mutant primary keratinocytes show decreased proliferation with an accumulation of cells in G1 phase in vitro, fitting to a TGFβ-induced cell-cycle arrest. Finally, inhibition of TGFβ signaling rescues the growth defect and the overexpression of p15INK4B by N-WASP-deficient keratinocytes in vitro, proving that the increase in TGFβ signaling and p15INK4B observed in *N-WASP*-null keratinocytes is functionally relevant. However, this relationship between loss of N-WASP and increased TGFβ signaling could only be observed if the knockout of N-WASP occurred in vivo. Knockout induction in vitro was not able to induce a strong alteration in cell growth or TGFβ signaling, underlining on the one hand the importance of in vivo analysis of signal transduction events, and indicating on the other hand that the N-WASP effect on TGFβ signaling is strongly regulated by environmental conditions.

The antiproliferative role of TGFβ in murine keratinocytes has been established using transgenic mouse strains expressing active or latent TGFβ under different promoters (Li et al., 2004; Sellheyer et al., 1993; Wang et al., 1999). However, due to neonatal lethality (Sellheyer et al., 1993), severe inflammation (Li et al., 2004) or a short observation period (Wang et al., 1999), no cyclic-alopecia phenotype was previously reported with these mice. Interestingly, however, injection of TGFβ1 into the back skin of mice reduces proliferation and increases apoptosis of hair follicle cells in vivo, thus promoting catagen (Foitzik et al., 2000). In the N-WASP mutant mice we also observed an increased frequency of apoptotic cells in the hair follicle in early catagen, which might contribute to the hair-loss phenotype. This similarity further corroborates our notion that the increased TGFβ signaling observed in N-WASP mutant mice contributes to their alopecia. Interestingly, we noticed that old N-WASP mutant mice displayed inflammation and hyperthickening of the foot pads, which might indicate an increased sensitivity towards mechanical stress (data not shown). Whether this late phenotype is related to inflammation-promoting effects of TGFβ signaling in keratinocytes is currently under investigation.

Although the molecular nature of the ‘hair cycle clock’ that drives hair-follicle cycling remains unclear (Paus and Foitzik, 2004), a recent landmark study has identified changing extrafollicular levels of BMP activity as a key parameter in determining wave-pattern formation and has indicated that intra- and extrafollicular oscillating signaling systems might cooperate to control both hair-follicle cycling and wave-pattern formation (Plikus et al., 2008). Our data do not yet allow one to conclude definitively that N-WASP-modulated TGFβ signaling, with its strong feedback regulation, is part of these oscillator systems (rather than being part of the molecular machinery that executes cyclic hair-follicle transformation changes dictated by the autonomous ‘hair cycle clock’ (Paus and Foitzik, 2004)). However, our data show that N-WASP-modulated TGFβ signaling qualifies as a hair-cycle regulating pathway, which can oscillate between different activation states, and suggest that it is closely linked with the ‘hair cycle clock’.

Because development and maintenance of the epidermis are normal in the absence of N-WASP, N-WASP appears to be dispensable for differentiation, cell-cell and cell-extracellular matrix contacts of interfollicular keratinocytes under physiological conditions. Our findings suggest furthermore that the role of N-

Journal of Cell Science

WASP in keratinocyte proliferation is dependent on environmental conditions. Although hair-follicle morphogenesis and onset of anagen are delayed in the absence of N-WASP, physiological proliferation in vivo is not detectably altered. In vivo, p21CIP protein is increased, whereas p15INK4B is not significantly altered. The increased p21CIP levels corresponded well to the delayed anagen onset because mice with reduced levels of p21CIP were reported to have a premature anagen onset (Mammucari et al., 2005). In vitro, however, p21CIP was hardly elevated and *N-WASP*-null cells showed instead a significant upregulation of p15INK4B and, in consequence, severe growth impairment.

It seems possible that N-WASP plays a more important role for keratinocyte proliferation in vivo under non-physiological conditions, which mimic the in vitro culture conditions. In this study we tested wound-induced hyperproliferation; however, we could not observe a defect in N-WASP knockout mice. In future studies, we will investigate other pathological conditions such as skin inflammation or skin tumor formation to reveal those conditions where N-WASP-dependent regulation of TGFβ signaling and p15INK4B might be crucial for keratinocyte growth in vivo. In skin cancer, increased TGFβ signaling was shown to inhibit the incidence and acceleration of carcinoma in skin, but also to promote metastasis formation of late tumors (Guasch et al., 2007; Bierie and Moses, 2006).

The normal wound closure of N-WASP-deficient mice in vivo indicated that N-WASP-mediated actin nucleation downstream of Cdc42 is not required for efficient re-epithelialization and that the increase in TGFβ signaling in *N-WASP*-null epidermis is not strong enough to inhibit wound closure (Werner and Grose, 2003).

Our study could not confirm a global role of N-WASP in RNA-polymerase-II-dependent gene expression (Wu et al., 2006a) because only few genes showed altered expression in primary *N-WASP*-null keratinocytes compared with control keratinocytes. For the same reason, it is unlikely that the suggested function of N-WASP in polymerization of nuclear actins has an important role in transcriptional regulation, as suggested before (Wu et al., 2006a). Although mice with a keratinocyte-restricted loss of the N-WASP regulator Cdc42 formed intra-epidermal blisters (Wu et al., 2006b), and inhibition of N-WASP in Caco-2 cells interfered with the maintenance of epithelial cell junctions (Otani et al., 2006), we could not find any evidence for an important function of N-WASP in cell-cell contacts of the epidermis. Also, preliminary studies on the formation of mature cell-cell junctions between *N-WASP*-null keratinocytes in vitro did not reveal an obvious defect (T.L. and C.B., unpublished data).

Our data suggest that N-WASP affects TGFβ signaling by regulating the amounts of TGFβ receptors. In vivo, TGFβRI is increased at the protein level, whereas TGFβRII is decreased. Because gene expression analysis of primary *N-WASP*-null keratinocytes did not reveal alterations in TGFβRI or TGFβRII transcripts, N-WASP most probably alters the turnover of the TGFβ receptors. Several studies indicate that such a regulation could be mediated by alterations in the endocytic uptake of the TGFβ receptors. Growth inhibition by TGFβ is mediated by a heterodimeric complex of TGFβRI and TGFβRII, which then phosphorylates Smad2 and Smad3, which activate the expression of the cell-cycle inhibitors p15INK4B and p21CIP (Ten Dijke et al., 2002). TGFβ receptors are constitutively internalized via clathrin-coated pits to endosomes, where they are recycled, or through caveolae, which leads to their degradation (Le Roy and Wrana, 2005). In most cell lines tested, clathrin-dependent internalization promotes TGFβ signaling by increased signaling in endosomes, due to increased amounts of the Smad2 anchor SARA through sequestration of SARA from the signaling-inhibiting caveolin-raft compartment, or by its reduced degradation (Le Roy and Wrana, 2005).

Previously, it was shown that N-WASP promotes the attachment of the Arp2/3 actin-polymerization machinery to clathrin-coated vesicles, thus speeding up internalization (Innocenti et al., 2005). Also, for clathrin-independent fluid phase endocytosis, N-WASP activation by SNX9 and phospholipids was found to be crucial (Yarar et al., 2007). Furthermore, on the basis of studies in yeast, it seems that inhibition of N-WASP slows down endosomal movements inside the cell (Chang et al., 2003). A hypothetical explanation for the observed phenotype in our study, therefore, would be that loss of N-WASP slows down uptake and endosomal transport of TGFβ receptors, thus prolonging the sojourn of the receptors in the endosomes and thereby increasing TGFβ signaling. Such delayed TGFβR trafficking has indeed recently been shown to explain the increased TGFβ signaling in cells treated with the anti-tumor drug CDDDO-Im (To et al., 2008). Further studies will have to investigate the extremely complex TGFβR trafficking and turnover in *N-WASP*-null keratinocytes to better understand this regulation.

N-WASP mediates Cdc42-dependent actin nucleation. The phenotype of mice lacking Cdc42 in keratinocytes, however, is quite different from the phenotype of the N-WASP mutant mice described here. In Cdc42-deficient mice, hair-follicle differentiation is stopped completely due to defective aPKCζ activation and increased β-catenin turnover (Wu et al., 2006c). Therefore, it is not possible to see more subtle defects in hair-follicle cycling as observed in the N-WASP mutant mice. The mild phenotype of mice lacking N-WASP in keratinocytes indicates in addition that the Cdc42-dependent regulation of aPKCζ activation and β-catenin signaling is independent of N-WASP.

In summary, our data provide the first evidence that regulation of the actin cytoskeleton by N-WASP involves cross-talk to TGFβR-mediated signaling in keratinocytes in vivo. This is important for keratinocyte proliferation, where increased TGFβ signaling conceivably delays the re-entry of hair follicles into the proliferative stage, and points towards previously unrecognized, important functions for N-WASP in epithelial biology.

## Materials and Methods

### Mouse strains

To obtain mice with a keratinocyte-restricted deletion of N-WASP, transgenic mice expressing Cre recombinase under the control of the K5 promoter (Ramirez et al., 2004) were intercrossed with mice homozygous for a floxed N-WASP allele (Lommel et al., 2001). All mice were on a 129Sv/C57Bl6 outbred background. All animal studies were carried out according to Danish rules of animal welfare.

### Histology, immunohistochemistry and electron microscopy

Hematoxylin-eosin (HE) staining, immunofluorescence staining and electron microscopy were performed as previously described (Chrostek et al., 2006). Alkaline phosphatase staining was performed by incubating cryosections with the alkaline phosphatase substrate NBT/BCIP (Roche) and counterstaining with Nuclear Fast Red solution (Sigma). Proliferation of keratinocytes in the epidermis was analyzed by BrdU incorporation as described previously (Chrostek et al., 2006). Images were taken at RT using a microscope (BX51) equipped 10× PlanC N (NA 0.25), 20× PlanC N (NA 0.40) and 40× UPlanSApo (NA 0.90) objectives, and a digital camera (Colorview IIIu) controlled by Cell^A software (version 2.3; all Olympus).

The following primary antibodies were used: K6, K10, K14 and loricrin (Covance), LN332 (γ2; kindly provided by Takako Sasaki, Max-Planck-Institute of Biochemistry, Martinsried, Germany), K33, K34, K71, K73, K75 and K82 (Langbein et al., 2003), Msx-2 (Santa Cruz Biotechnology), cleaved caspase-3 (Asp175) and p44/42 MAP kinase (Cell Signaling Technology), versican (kindly provided by Dieter Zimmermann, University Hospital Zurich, Zurich, Switzerland), paxillin (BD) and FITC-conjugated CD49f (integrin α6 chain; BD Biosciences).

Journal of Cell Science

As secondary reagents Cy3-conjugated goat anti-rabbit IgG (Jackson ImmunoResearch) and Alexa-Fluor-594-conjugated goat anti-guinea pig IgG (Invitrogen) antibodies were used. F-actin was visualized by Alexa-Fluor-488-coupled phalloidin (Invitrogen). Nuclear DNA was visualized with DAPI (Sigma) or Draq5 (Biostatus Limited).

For p21CIP staining, 6-μm thick paraffin sections were unmasked, blocked with the MOM kit (Vector laboratories) and incubated with mouse anti-p21CIP antibody (F-5; Santa Cruz Biotechnology). After amplification with the TSA biotin system (PerkinElmer), p21CIP was detected with Texas red avidin DCS (Vector Laboratories).

Images were analyzed at RT by confocal microscopy using a TCS SP2 system with a DM RXA2 microscope, equipped with 20× HC PL Apo (NA 0.70), 40× HCX PL APO (NA 1.25-0.75) and 63× HCX PL APO (NA 1.40-0.60) objectives, controlled by Leica Microsystems confocal software (version 2.61 Build 1537; all Leica Microsystems).

### Biochemical analysis

Western blotting was performed according to standard protocols and results quantified using TotalLab TL100 software (Nonlinear Dynamics). Tubulin was used to normalize for different protein amounts.

The following primary antibodies were used: N-WASP (Lommel et al., 2001), p44/42 MAP kinase (Erk), phosphorylated p44/42 MAP kinase (Erk-*P*), phosphorylated Smad2 and Smad1/5/8 (all Cell Signaling Technology), p21CIP (clone F-5; Santa Cruz Biotechnology), HES-1 (Chemicon), TGFβ RI/ALK-5, TGFβ RII (both RandD Systems), TGFβ1,2,3, Smad6/7 (N19; all Santa Cruz Biotechnology), p15 INK4B (Cell Signaling Technology) and tubulin (Y/L1/2). Secondary reagents used were horseradish-peroxidase-coupled goat anti-rabbit, anti-rat and anti-mouse antibodies (Jackson ImmunoResearch). All reagents were used under the conditions and at the concentrations suggested by the manufacturers.

### Primary keratinocyte culture, adhesion assay, microarray and qRT-PCR

Isolation of primary keratinocytes from adult mice and subsequent in vitro culture was carried out as described previously (Chrostek et al., 2006). For microarray analysis of primary keratinocytes, samples were prepared according to standard protocols. Hybridization to GeneChip Mouse Genome 430 2.0 Array (Affymetrix) was carried out at the Copenhagen University Hospital Microarray Center.

qRT-PCR was performed on the Applied Biosystems 7300 Real Time PCR system using SYBR green incorporation following standard protocols.

### FACS analysis

Freshly isolated primary keratinocytes were allowed to grow to subconfluency and were replated to ensure equal density. After 24 hours, cells were harvested and DNA was stained with propidium iodide and measured with a FACSCalibur flow cytometer using CellQuest Pro software (BD Biosciences).

### Keratinocyte proliferation assay

Subconfluent primary keratinocytes were plated at equal density in 96-well plates in growth medium and crystal violet staining was performed on four consecutive days. Absorbance values were taken as a measure for the growth of the cells.

To test the effect of TGFβ inhibition, medium was changed 4 hours after plating to medium containing TGFβ RI kinase inhibitor II (Calbiochem) at concentrations varying from 0 to 2500 ng/ml (constant amount of vehicle). Medium was changed daily to ensure constant inhibitor concentration.

### Adhesion assay

For adhesion assay, 96-well plates were coated for 2 hours at 37°C with 30 μg/ml collagen type I (Inamed Biomaterials), 10 μg/ml fibronectin (Biological Industries BioMedical) in phosphate-buffered saline (PBS), and blocked with 1% BSA in PBS for 90 minutes at 37°C. Keratinocytes were seeded and allowed to attach to the wells for 1 hour at 34°C. Non-adherent cells were washed away with PBS. Attached cells were fixed with 70% ethanol and stained with 5 mg/ml crystal violet in 20% methanol. After washing away excess dye and letting the plates dry in air, 1% SDS in PBS was added to the wells and absorbance was measured at 590 nm with a plate reader (Bio-Tek Instruments).

### Wound healing

Full-thickness wounds (two per mouse) were created on the back skin of mice using a 4-mm biopsy punch. Three days after wounding, mice were killed and wounds were excised, bisected and fixed in 4% paraformaldehyde overnight. HE-stained paraffin sections of the wounds were then analyzed for wound width.

### In vitro induction of N-WASP deficiency

Primary keratinocytes were isolated from adult N-WASP fl/fl mice and transfected with pRRLSIN-GFP or pRRLSIN-CRE-IRES-EGFP (kindly received from Didier Trono, EPFL, Lausanne, Switzerland) using *Trans*IT-Keratinocyte Transfection Reagent (Mirus) to induce transient GFP expression or EGFP and Cre recombinase expression, respectively. At 48 hours after transfection, cells were either replated and analyzed on a FACSCalibur flow cytometer (BD Biosciences) at the given time-points, or sorted using a FacsAria Cell Sorting System (BD Biosciences) to isolate transfected cells and replated to be lysed at later time-points.

### Statistical analysis

Data are expressed as means ± s.d., with error bars representing s.d. Statistical significance was determined by two-tailed Student's *t*-test and significant differences are indicated by asterisks.

We thank Reinhard Fässler for his very generous support, Takako Sasaki and Dieter Zimmermann for antibodies, Didier Trono for lentiviral vectors, Pierce Lalor for technical help, David Wallach for discussion, and Rehannah Borup for help with the microarray. This work was funded by the Max Planck Society, the German Research Council (Pa 345/12-1), the Novo Nordisk Foundation and the Friis Foundation.

Supplementary material available online at
http://jcs.biologists.org/cgi/content/full/123/1/128/DC1

## References

**Bierie, B. and Moses, H. L.** (2006). Tumour microenvironment: TGFbeta: the molecular Jekyll and Hyde of cancer. *Nat. Rev. Cancer* **6**, 506-520.

**Chang, F. S., Stefan, C. J. and Blumer, K. J.** (2003). A WASp homolog powers actin polymerization-dependent motility of endosomes in vivo. *Curr. Biol.* **13**, 455-463.

**Cho, Y. S., Bae, J. M., Chun, Y. S., Chung, J. H., Jeon, Y. K., Kim, I. S., Kim, M. S. and Park, J. W.** (2008). HIF-1 alpha controls keratinocytes proliferation by up-regulating p21(WAF/Cip1). *Biochim. Biophys. Acta.* **1783**, 323-333.

**Chrostek, A., Wu, X., Quondamatteo, F., Hu, R., Sanecka, A., Niemann, C., Langbein, L., Haase, I. and Brakebusch, C.** (2006). Rac1 is crucial for hair follicle integrity but is not essential for maintenance of the epidermis. *Mol. Cell. Biol.* **26**, 6957-6970.

**Co, C., Wong, D. T., Gierke, S., Chang, V. and Taunton, J.** (2007). Mechanism of actin network attachment to moving membranes: barbed end capture by N-WASP WH2 domains. *Cell* **128**, 901-913.

**Dennis, G., Sherman, B. T., Hosack, D. A., Yang, J., Gao, W., Lane, H. C. and Lempicki, R. A.** (2003). DAVID: database for annotation, visualization, and integrated discovery. *Genome Biol.* **4**, P3.

**Foitzik, K., Lindner, G., Mueller-Roever, S., Maurer, M., Botchkareva, N., Botchkarev, V., Handjiski, B., Metz, M., Hibino, T., Soma, T. et al.** (2000). Control of murine hair follicle regression (catagen) by TGF-beta1 in vivo. *FASEB J.* **14**, 752-760.

**Fuchs, E.** (2007). Scratching the surface of skin development. *Nature* **445**, 834-842.

**Guasch, G., Schober, M., Pasolli, H. A., Conn, E. B., Polak, L. and Fuchs, E.** (2007). Loss of TGFbeta signaling destabilizes homeostasis and promotes squamous cell carcinomas in stratified epithelia. *Cancer Cell* **12**, 313-327.

**Hempel, N., How, T., Cooper, S. J., Green, T. R., Dong, M., Copland J. A., Wood, C. G. and Blobe, G. C.** (2008). Expression of the type III TGF-beta receptor is negatively regulated by TGF-beta. *Carcinogenesis* **29**, 905-912.

**Innocenti, M., Gerboth, S., Rottner, K., Lai, F. P. L., Hertzog, M., Stradal, T. E. B., Frittoli, E., Didry, D., Polo, S., Disanza, A. et al.** (2005). Abi1 regulates the activity of N-WASP and WAVE in distinct actin-based processes. *Nat. Cell Biol.* **7**, 969-976.

**Langbein, L. and Schweizer, J.** (2005). Keratins of the human hair follicle. *Int. Rev. Cytol.* **243**, 1-78.

**Langbein, L., Rogers, M. A., Praetzel, S., Winter, H. and Schweizer, J.** (2003). K6irs1, K6irs2, K6irs3, and K6irs4 represent the inner-root-sheath-specific type II epithelial keratins of the human hair follicle. *J. Invest. Dermatol.* **120**, 512-522.

**Le Roy, C. and Wrana J. L.** (2005). Clathrin- and non-clathrin-mediated endocytic regulation of cell signalling. *Nat. Rev. Mol. Cell. Biol.* **6**, 112-126.

**Li, A. G., Wang, D., Feng, X. and Wang, X.** (2004). Latent TGFbeta1 overexpression in keratinocytes results in a severe psoriasis-like skin disorder. *EMBO J.* **23**, 1770-1781.

**Lommel, S., Benesch, S., Rottner, K., Franz, T., Wehland, J. and Kühn, R.** (2001). Actin pedestal formation by enteropathogenic Escherichia coli and intracellular motility of Shigella flexneri are abolished in N-WASP-defective cells. *EMBO Rep.* **2**, 850-857.

**Ma, L., Liu, J., Wu, T., Plikus, M., Jiang, T., Bi, Q., Liu, Y., Müller-Röver, S., Peters, H., Sundberg, J. P. et al.** (2003). 'Cyclic alopecia' in Msx2 mutants: defects in hair cycling and hair shaft differentiation. *Development* **130**, 379-389.

**Mammucari, C., Tommasi di Vignano, A., Sharov, A. A., Neilson, J., Havrda, M. C., Roop, D. R., Botchkarev, V. A., Crabtree, G. R. and Dotto, G. P.** (2005). Integration of Notch 1 and calcineurin/NFAT signaling pathways in keratinocyte growth and differentiation control. *Dev. Cell* **8**, 665-676.

**Millard, T. H., Sharp, S. J. and Machesky, L. M.** (2004). Signalling to actin assembly via the WASP (Wiskott-Aldrich syndrome protein)-family proteins and the Arp2/3 complex. *Biochem. J.* **380**, 1-17.

**Mizutani, K., Miki, H., He, H., Maruta, H. and Takenawa, T.** (2002). Essential role of neural Wiskott-Aldrich syndrome protein in podosome formation and degradation of extracellular matrix in src-transformed fibroblasts. *Cancer Res.* **62**, 669-674.

**Müller-Röver, S., Handjiski, B., van der Veen, C., Eichmüller, S., Foitzik, K., McKay, I. A., Stenn, K. S. and Paus, R.** (2001). A comprehensive guide for the accurate classification of murine hair follicles in distinct hair cycle stages. *J. Invest. Dermatol.* **117**, 3-15.

**Niessen, C. M.** (2007). Tight junctions/adherens junctions: basic structure and function. *J. Invest. Dermatol.* **127**, 2525-2532.

**Otani, T., Ichii, T., Aono, S. and Takeichi, M.** (2006). Cdc42 GEF Tuba regulates the junctional configuration of simple epithelial cells. *J. Cell Biol.* **175**, 135-146.

**Pardali, K., Kowanetz, M., Heldin, C. and Moustakas, A.** (2005). Smad pathway-specific transcriptional regulation of the cell cycle inhibitor p21(WAF1/Cip1). *J. Cell Physiol.* **204**, 260-272.

**Paus, R. and Foitzik K.** (2004). In search of the "hair cycle clock": a guided tour. *Differentiation* **72**, 489-511.

**Paus, R., Müller-Röver, S., Van Der Veen, C., Maurer, M., Eichmüller, S., Ling, G., Hofmann, U., Foitzik, K., Mecklenburg, L. and Handjiski, L. B.** (1999). A comprehensive guide for the recognition and classification of distinct stages of hair follicle morphogenesis. *J. Invest. Dermatol.* **113**, 523-532.

**Pinyol, R., Haeckel, A., Ritter, A., Qualmann, B. and Kessels, M. M.** (2007). Regulation of N-WASP and the Arp2/3 complex by Abp1 controls neuronal morphology. *PLoS ONE* **2**, e400.

**Plikus, M. V., Mayer, J. A., de la Cruz, D., Baker, R. E., Maini, P. K., Maxson, R. and Chuong, C.** (2008). Cyclic dermal BMP signalling regulates stem cell activation during hair regeneration. *Nature* **451**, 340-344.

**Pollard, T. D. and Borisy, G. G.** (2003). Cellular motility driven by assembly and disassembly of actin filaments. *Cell* **112**, 453-465.

**Ramirez, A., Page, A., Gandarillas, A., Zanet, J., Pibre, S., Vidal, M., Tusell, L., Genesca, A., Whitaker, D. A. et al.** (2004). A keratin K5Cre transgenic line appropriate for tissue-specific or generalized Cre-mediated recombination. *Genesis* **39**, 52-57.

**Rangarajan, A., Talora, C., Okuyama, R., Nicolas, M., Mammucari, C., Oh, H., Aster, J. C., Krishna, S., Metzger, D., Chambon, P. et al.** (2001). Notch signaling is a direct determinant of keratinocyte growth arrest and entry into differentiation. *EMBO J.* **20**, 3427-3436.

**Reynisdóttir, I., Polyak, K., Iavarone, A. and Massagué, J.** (1995). Kip/Cip and Ink4 Cdk inhibitors cooperate to induce cell cycle arrest in response to TGF-beta. *Genes Dev.* **9**, 1831-1845.

**Sellheyer, K., Bickenbach, J. R., Rothnagel, J. A., Bundman, D., Longley, M. A., Krieg, T., Roche, N. S., Roberts, A. B. and Roop, D. R.** (1993). Inhibition of skin development by overexpression of transforming growth factor beta 1 in the epidermis of transgenic mice. *Proc. Natl. Acad. Sci. USA* **90**, 5237-5241.

**Snapper, S. B., Takeshima, F., Antón, I., Liu, C. H., Thomas, S. M., Nguyen, D., Dudley, D., Fraser, H., Purich, D., Lopez-Ilasaca, M. et al.** (2001). N-WASP deficiency reveals distinct pathways for cell surface projections and microbial actin-based motility. *Nat. Cell Biol.* **3**, 897-904.

**Stenn, K. S. and Paus, R.** (2001). Controls of hair follicle cycling. *Physiol. Rev.* **81**, 449-494.

**Ten Dijke, P., Goumans, M., Itoh, F. and Itoh, S.** (2002). Regulation of cell proliferation by Smad proteins. *J. Cell Physiol.* **191**, 1-16.

**To, C., Kulkarni, S., Pawson, T., Honda, T., Gribble, G. W., Sporn, M. B., Wrana, J. L. and Di Guglielmo, G. M.** (2008). The synthetic triterpenoid 2-cyano-3,12-dioxooleana-1,9-dien-28-oic acid-imidazolide alters transforming growth factor beta-dependent signaling and cell migration by affecting the cytoskeleton and the polarity complex. *J. Biol. Chem.* **283**, 11700-11713.

**Wang, X. J., Liefer, K. M., Tsai, S., O'Malley, B. W. and Roop, D. R.** (1999). Development of gene-switch transgenic mice that inducibly express transforming growth factor beta1 in the epidermis. *Proc. Natl. Acad. Sci. USA* **96**, 8483-8488.

**Werner, S. and Grose, R.** (2003). Regulation of wound healing by growth factors and cytokines. *Physiol. Rev.* **83**, 835-870.

**Wu, X., Yoo, Y., Okuhama, N. N., Tucker, P. W., Liu, G. and Guan, J.** (2006a). Regulation of RNA-polymerase-II-dependent transcription by N-WASP and its nuclear-binding partners. *Nat. Cell Biol.* **8**, 756-763.

**Wu, X., Quondamatteo, F. and Brakebusch, C.** (2006b). Cdc42 expression in keratinocytes is required for the maintenance of the basement membrane in skin. *Matrix Biol.* **25**, 466-474.

**Wu, X., Quondamatteo, F., Lefever, T., Czuchra, A., Meyer, H., Chrostek, A., Paus, R., Langbein, L. and Brakebusch, C.** (2006c). Cdc42 controls progenitor cell differentiation and beta-catenin turnover in skin. *Genes Dev.* **20**, 571-585.

**Yarar, D., Waterman-Storer, C. M. and Schmid, S. L.** (2007). SNX9 couples actin assembly to phosphoinositide signals and is required for membrane remodeling during endocytosis. *Dev. Cell* **13**, 43-56.

Journal of Cell Science